**Title**
Mechanism of Outer Mitochondrial Membrane Associated Degradation Investigated by BioID of SLC25A46.



**Author**
Batty, Luke Daniel

**Publication Date**
2017

UNIVERSITY OF CALIFORNIA

Los Angeles

# Mechanism of Outer Mitochondrial Membrane Associated Degradation Investigated by BioID of SLC25A46.

A thesis submitted in partial satisfaction of the requirements for the degree Master of Science in Biochemistry, Molecular and Structural Biology

by

Luke Daniel Batty

2017

ABSTRACT OF THE THESIS

Mechanism of Outer Mitochondrial Membrane
Associated Degradation Investigated by BioID of
SLC25A46.

by

Luke Daniel Batty

Master of Science in Biochemistry, Molecular and
Structural Biology

University of California, Los Angeles, 2017

Professor Carla Marie Koehler, Chair

The selective removal of damaged or misfolded outer mitochondrial membrane (OMM) proteins is a necessary process to avoid total organelle destruction by mitophagy. This sensing system is called outer mitochondrial membrane associated degradation (OMMAD) and is poorly understood. OMMAD uses the ubiquitin proteasome system (UPS), much like endoplasmic reticulum associated degradation (ERAD), but the specific players composing the pathway are unknown. In this study, we sought to identify some of these components by appending a promiscuous biotin ligase, BirA, to the OMM protein SLC25A46, known to be degraded by this pathway when mutated at a single point. As controls for unspecific biotinylation, we created BirA-MCherry and Mid49-BirA constructs, for the cytosol and OMM, respectively. Mass spectrometry analysis led to the discovery of a potentially novel pathway for OMM protein

degradation via the ER. This conclusion is supported by Percoll gradient centrifugation studies indicating the presence of mutated SLC25A46 in the endoplasmic reticulum (ER).

The thesis of Luke Daniel Batty is approved.

Catherine F. Clarke

Alexander M. van der Bliek

Carla Marie Koehler, Committee Chair

University of California, Los Angeles

2017

TABLE OF CONTENTS


| | PAGE |
|---|---|
| ABSTRACT | ii |
| COMMITTEE PAGE | iv |
| TABLE OF CONTENTS | v |
| LIST OF FIGURES | vi |
| LIST OF TABLES | vii |
| INTRODUCTION | 1 |
| MATERIALS AND METHODS | 5 |
| RESULTS | 9 |
| DISCUSSION | 18 |
| REFERENCES | 21 |

LIST OF FIGURES

PAGE

FIGURE 1 12

FIGURE 2 13

FIGURE 3 14

FIGURE 4 15

FIGURE 5 17

LIST OF TABLES

PAGE

TABLE 1 16

## Introduction

In every eukaryotic cell, mitochondria are necessary to produce the ATP the cell uses as chemical energy, along with the precursors to most all metabolic pathways active in the cell (Dudek et al., 2013). Mitochondria have conserved pathways for protein import that are generally well characterized (Lenaz, 1998). This consists of the translocase of the outer membrane (TOM) and translocase of the inner membrane (TIM) complexes working in concert with other import machinery such as the sorting and assembly machinery (SAM) and mitochondrial intermembrane space import and assembly (MIA) complexes to correctly localize proteins to the major subdomains of the organelle: the outer membrane (OM), intermembrane space (IMS), inner membrane (IM), and matrix (Pusnik et al., 2009).

Metabolite import into the matrix requires the action of large β-barrel porins in the OM and specific α-helical mitochondrial carriers in the IM. The SLC25 family of proteins is the largest group of transmembrane transporters found in the IM. The family is responsible for the transport of essential intermediates and cofactors such as ornithine, aspartate, glutamate, S-adenosylmethionine, ADP, ATP, coenzyme A, FAD, $NAD^+$, phosphate, citrate, and oxaloacetate (Palmieri, 2014). The 24 known subfamilies, defined by what they import and export, are present in all eukaryotes, with the exception of five plant and yeast specific members. The SLC25 family is characterized by three repeat domains of two hydrophobic transmembrane helices connected by a hydrophilic loop, usually extending into the matrix (Palmieri, 2014).

Metabolite import will increase or decrease depending, in large part, on the current dynamics of the mitochondria (Wai and Langer, 2016). Mitochondria are in a constant state of fusion and fission to respond to the metabolic needs of the cell, with fission more prevalent in metabolite poor environments and fusion more likely in metabolite-rich environments (Liesa and

Shirihai, 2013). These processes of mitochondrial dynamics are instituted by fusion proteins such as mitofusin 1 (MFN1) and MFN2, or the fission protein dynamin-related protein 1 (DRP1) (Chen et al., 2003).

We have identified a novel mitochondrial outer membrane protein, SLC25A46, that functions in mitochondrial dynamics (Wan et al., 2016). SLC25A46 is the only family protein found in the OM as opposed to the normal location in the IM, and this raises questions about its function (Abrams et al., 2015). Previous studies have implicated a role of SLC25A46 in the development of neuronal tissue at the organismal level, as well as involvement in mitochondrial dynamics at the cellular level (Abrams et al., 2015). When there is a loss of function in this protein, there is an observed hyperfusion of mitochondria, leading to many metabolic issues and retarded tissue development (Janer et al., 2016). In the nonfatal mutations of SLC25A46 studied by Abrams et al. (G249D and E335D), the patients exhibited optic atrophy, axonal peripheral neuropathy, and cerebellar atrophy. However, the specific biochemical mechanisms responsible for these phenotypes are still unknown.

Mitochondrial protein quality control and turnover pathways are vital processes necessarily connected to protein and metabolite import, processing incoming proteins using the ATP produced by metabolites (Koppen and Langer, 2007). Within both the IMS and the matrix, there are well known processing peptidases, such as mitochondrial processing peptidase (MPP) and mitochondrial intermediate peptidase (MIP), responsible for cleaving off the mitochondrial targeting sequences of newly imported proteins, among other functions (Ou et al., 1989; Kalousek et al., 1992). Besides processing, there are two other classes of proteases within the IMS and matrix: ATP-dependent proteases and oligopeptidases. ATP-dependent proteases are responsible for the recognition and degradation of misfolded or damaged proteins within the

IMS, IM, and matrix, accomplished through their P-loop ATPase domains (Van Dyck and Langer, 1999). This results in large oligopeptides that are converted into free amino acids by the oligopeptidases, completing the turnover pathways of the inner mitochondria (Young et al., 2001).

In contrast to those of the IMS and matrix, little is known about protein quality control and turnover pathways for the assembly of outer membrane proteins (Karbowski and Youle, 2011). An outer membrane protein that is misfolded requires a sensing system to trigger selective removal and degradation from the outer membrane without triggering degradation of the entire organelle by a pathway known as mitophagy. The components that regulate this pathway have not been identified. From preliminary studies, degradation requires the ubiquitin-proteasome system (UPS), much like the endoplasmic reticulum associated degradation (ERAD) pathway (Karbowski and Youle, 2011). In ERAD, the sensing system involves the function of ubiquitin ligases that will create a polyubiquitin tail on the target protein. In mammals, these ubiquitin ligases are HRD1 and GP78, which function on separate substrates, depending on the location of the damage or misfolding (Burr et al., 2013; Ruggiano et al., 2014). This process is facilitated by the recognition machinery, which includes the binding immunoglobulin protein (BiP) chaperone complex, and the luminal elements of the membrane bound E3 ubiquitin ligases. Once recognized, the polyubiquitinated signal leads to membrane removal by the P97 complex and the SEC61 retrotranslocon, followed by proteasomal degradation (Ruggiano et al., 2014). Potential candidates that function as sensors to signaling OM protein misfolding are the OM ubiquitin ligases MARCH5, MULAN, and Mdm30, all of which function to control the levels of key mitochondrial dynamics effectors (Neutzner et al., 2007).

Recently, evidence has suggested that SLC25A46 is degraded by this mechanism. A specific point mutation in one of the membrane spanning domains of SLC25A46 results in rapid and selective degradation without damaging the mitochondrial network (Steffen et al., 2017). It has been demonstrated to be involved in the regulation of MFN2 oligomerization, with reduced levels of SLC25A46 leading to increased occurrence of oligomerization, providing a biochemical mechanism to the mitochondrial hyperfusion observed in the past (Wan et al., 2016). This connection to mitochondrial dynamics is supported by data demonstrating SLC25A46 is ubiquitinated by the dual, redundant function of MARCH5 and MULAN (Steffen et al., 2017).

The goal of this study is to use SLC25A46 to characterize the mechanism of this targeted degradation, a process that is referred to as outer mitochondrial membrane assisted degradation (OMMAD) (Karbowski and Youle, 2011). Because SLC25A46 mutation activates the sensing machinery for the OM, we propose to utilize the BioID system to identify some of these components. In the BioID system, a biotin ligase enzyme is appended to the N-terminus of SLC25A46, and this construct is transfected into tissue culture to generate stable cell lines. Once these lines have been optimized for expression, the biotinylation products will be identified through streptavidin-associated affinity purification, followed by mass spectroscopy. Suspected components of OMMAD will then be verified through biochemical methods.

## Materials and Methods

*Cloning Procedures*

The BirA*-Flag-MCherry construct was kindly provided by Dr. James Wohlschlegel (UCLA). BirA*-Flag-SLC25A46, BirA*-Flag-SLC25A46 (L341P), and Mid49-Flag-BirA* were generated by Gibson fusion cloning into the vector pcDNA5/FRT/TO (for stable expression, Clontech) after digestion with DpnI and XhoI (New England Biolabs). Template plasmids for SLC25A46, SLC25A46 (L341P), and Mid49 were kindly provided by Dr. Janos Steffen (UCLA). Primer sequences used:

-SLC25A46 (WT and L341P)

For) 5'- CGGGGTACCATGCATCCGCGGCGCCCG -3',

Rev) 5'- AACGGGCCCTCTAGACTCGAGTCAAATGTTATTTTGAAGAAG -3';

-Mid49

For) 5'- GTTTAAACTTAAGCTTGGTACCATGGCAGAGTTCTCCCAGAAAC -3',

Rev) 5'-ATCACCAGAGCCTCCCTCGAGCGGCCGCGCGAGCAGCCCCTCGGGCTCCTG-3'. All constructs were verified by sequencing (Genewiz).

*Culture and Transfection of HEK293 cells*

Human Embryonic Kidney (HEK) 293 T-REx Flp-In cells were grown in DMEM media containing 10% FBS (Atlanta Biological) and 10mm Pennicillin/Streptomycin (Fisher). Cells were seeded at 106 cells /well in a six-well plate. Plasmids were transfected using BioT transfection reagent (Bioland) for 48 hours. After transfection, cells were selected with 2ug/well Puromycin (Life Technologies) for 48 hours.

*Tissue Culture Sample Growth Procedure*

BioID HEK293 T-REx Flp-In cell lines (BirA-MCherry, Mid49-BirA, BirA-WT, and BirA-L341P) were seeded on 10cm dishes at $1x10^6$ cells/plate. These were allowed to grow to 75% confluence and then induced with 10ng/µL doxycycline within or without the presence of 10µM Biotin for 24 hours. These plates were then harvested via scraping.

*Blue Native PAGE and Western blot*

Resuspended HEK293 cells were agitated in a Teflon dounce and separated into crude mitochondria and cytosol by successive centrifugations first at 800g, then at 10,000g. Crude mitochondria and cytosol were run on a 10% SDS-PAGE gel or a 4-12% acrylamide gradient gel, and transferred to a nitrocellulose/PVDF membrane. Membrane was incubated overnight with primary antibody [SLC25A46 (Proteintech); FLAG (Biolegend); Streptavidin-HRP (Cell Signaling); MFN2 (Sigma Aldrich); TOMM40 polyclonal antibodies were raised against recombinant proteins (Pacific Immunology)], washed, then probed with secondary antibody and visualized with ECL/ECL Plus/substrate (Thermo Fisher).

*BioID and Cell Lysis*

BioID HEK293 T-REx Flp-In cell lines were seeded on 4x15cm dishes at $2.5x10^6$ cells/plate and allowed to grow for 48 hours. They were then induced for 24 hours with 10 ng/µL doxycycline, followed by a further 24 hour induction in the presence of 10 µM biotin. These cells were harvested by scraping and lysed in 8M urea, 2% SDS, 100 mM Tris (pH 8). Cells were sonicated, centrifuged, and normalized via Pierce BCA kit.

*Bead Preparation and Affinity Purification*

High-capacity streptavidin agarose slurry (Thermo-Fisher; 20359) were reductively methylated as in the Reductive Alkylation Kit from Hampton Research (HR2-434). Cell lysate was introduced to alkylated beads and allowed to incubate for 2 hours at RT. Beads were then washed with the following in succession: Lysis Buffer (8 M urea, 2% SDS, 100 mM Tris [pH 8]), Wash II (8 M urea, 2% SDS, 500 mM NaCl, 100 mM Tris [pH 8]), Wash III (8 M urea, 0.2% SDS, 500 mM NaCl, 5% ethanol, 5% isopropanol, 100 mM Tris [pH 8]), and Digestion Buffer (8 M urea, 100 mM Tris [pH 8.5]).

*Mass Spectrometry*

BioID samples were resuspended in 100 mM Tris pH 8.5, 8M urea and digested on-bead by the sequential addition of lys-C and trypsin proteases (Wohlschlegel, 2009). After desalting, each sample analyzed by LC-MS/MS on a Thermofisher Fusion Lumos Orbitrap mass spectrometer coupled to a Dionex Ultimate 3000 ultra-high pressure liquid chromatography system (Senko et al., 2013). Online peptide separations were performed on a 75 uM outer diameter fused silica capillary column with an integrated emitter packed in-house with 25 cm of 1.9uM C18 particles (Dr Maisch) using a 140 minute linear gradient of increasing acetonitrile. Data was collected on the Lumos mass spectrometer in a data-dependent manner consisting of 3 second cycle times composed of a 120K resolution full MS orbitrap scan (m/r scan range = 400 – 1600) followed by 15K MS/MS orbitrap scans of the most abundant ions from the preceding full MS scan. RAW MS/MS data was converted to mzml format using Proteowizard msconvert and then searched against a Uniprot database consisting of all annotated human ORFs using the MSGF+ search algorithm (Adusumilli and Mallick, 2017; Kim and Pevzner, 2014). Peptide- and protein-level

filtering will be done using FDR cutoffs of 0.01 as estimated using a decoy database approach and the percolator and FIDO algorithms, respectively (Kall et al., 2007; Serang et al., 2010). Label-free quantitation of identified peptides across all samples was performed MS1-level extracted ion chromatograms generated by the Skyline algorithm (Schilling et al., 2012), peak detection according to mProphet (Reiter et al., 2011), and statistical validation by MSStats (Choi et al., 2014).

*Percoll Gradient Centrifugation*

Crude mitochondria and cytosolic fractions were obtained as above. The ER fraction was obtained by ultracentrifugation at 100,000g at 4°C for one hour, and the pellet was resuspended by teflon dounce and pestel. The Percoll gradient was created by layering 5.5 mL 24% Percoll over 5.5 mL 40% Percoll. Crude mitochondria were run over this gradient at 20,000 rpm at 4°C for 40 minutes. This produced the second crude mitochondrial fraction and the pure mitochondrial fraction.

## Results

*BirA Recombinant Cell Lines are Optimized for Streptavidin Affinity Purification*

To determine whether SLC25A46 degradation could be used to identify the components of the OMMAD pathway, the promiscuous biotin ligase BirA was appended to the N-terminus of mutant (L341P) and native (WT) SLC25A46 to create recombinant proteins. To act as controls for unspecific biotinylation, the common cytosolic protein MCherry was tagged at the N-terminus, and common OM protein Mid49 was tagged at the C-terminus. These constructs were transfected into HEK 293 TRex FlpIn SLCKO cell lines we previously produced through Cas9-CRISPR. After screening for single cell colonies, these cell lines were subjected to standard optimization.

The first step in optimizing recombinant cell lines is inducibility, and a titration of the inducer. The BirA constructs are designed to be induced by doxycycline. Titrating from a concentration of 5-50 ng/µL, it was determined that the optimal concentration of inducer was 10 ng/µL (Fig. 1A-D). This concentration produces sufficient protein but is not saturating. Despite blotting defects (Fig. 1B, lane 4), it was clear that all recombinant cell lines were sufficiently inducible.

We next sought to determine whether the cell lines were capable of biotinylation in the presence of biotin. It was seen that only when induced in doxycycline for 24 hours in the presence of biotin, the MCherry, Mid49, and WT cell lines were noticeably capable of biotinylation (Fig. 2). The L341P cell line was not capable of noticeable biotinylation, which we postulate is due to the rapid turnover of the mutant protein.

Because the correct localization of the recombinant proteins is vital for the success of the BioID assay, we determined the subcellular localization of each BirA construct. BirA-MCherry

was appropriately localized to the cytosol, while Mid49-BirA and BirA-WT were found in the mitochondrial fraction (Fig. 3). Unfortunately, despite multiple repeats at high exposure, the BirA-L341P location could not be confirmed. This could be repeated blotting failure, or a symptom of the high turnover rate of the mutant protein *in vivo*.

Now that we were confident that the cell lines were inducible, could biotinylate, and were correctly localized, we determined whether the SLC25A46 constructs were properly functional. It is already established (Steffen et al., 2017) that SLC25A46 loss of function leads to an increase of MFN2 complexes, so we used this fact to assay the functionality of the cell lines. The BirA-WT protein could successfully decrease the MFN2 complexes after induction (Fig. 4A). Strangely, the BirA-L341P construct was also shown to reduce the MFN2 accumulation, which is usually not the case due to rapid turnover. In addition, it was shown that induction of each SL25A46 construct in the presence of biotin led to the specific biotinylation of proteins in the cytosol (L341P) and mitochondrial (WT) fractions (Fig. 4B). The fact that BirA-L341P mainly biotinylates in the cytosol could suggest that the protein is mainly in a state of active proteasomal degradation, explaining the difficulty in subcellular localization.

*SLC25A46 Associates with ER Proteins Before Degradation*

Following the creation of verified BioID-appropriate tissue culture systems, the BioID approach was used to perform streptavidin affinity purification. This will allow the separation and purification of all biotinylated proteins within the cell, including those biotinylated by the recombinant proteins. Once this procedure was performed and verified to be successful, the samples were sent to the James Wohlschlegel lab for mass spectrometry and analysis.

The mass spectrometry seems to be robust, containing over 2500 separate proteins identified in the raw data collected though two biological replicates, along with two technical replicates each (Supplementary Materials). After analyzing the raw data manually, a pattern in the mutant construct data became clear, showing specificity for ER membrane and luminal proteins (Table 1). Of the highest hits were proteins such as protein disulfide isomerase (PDI), 78 kDa glucose-regulated protein (GRP78), and hypoxia up-regulated protein 1 (HYOU1), where there was 4 to 10-fold difference between the mutant NSAF value and that of the controls. These are all canonical members of the well characterized BiP chaperone complex, responsible for quality control processes of the ER lumen, specifically of those proteins that do not contain signals for glycosylation (Kleizen and Braakman, 2004). This suggests that SLC25A46 is somehow associated with the ER lumen before it is degraded by the proteasome.

In addition to unexpected members of ER quality control, there was also observed to be a significant marking of the proteasome, specifically the 26S regulatory subunit and the 26S non-ATPase domain, which is consistent with the BirA construct's biotinylation during degradation. This indicates that our experimental method was successful in marking the components of SLC25A46's degradation pathway.

To confirm the reliability of the mass spectrometry data we obtained that indicated the interaction of SLC25A46-L341P with the ER, Percoll gradient centrifugation was performed to more completely separate pure fractions of subcellular compartments. Once pure ER was separated from mitochondria, it was shown that SLC25A46-L341P is preferentially found in the ER fraction, while wildtype SLC25A46 is found only in the mitochondria (Fig. 5). This confirms the report of the mass spectrometry data, which indicated that the L341P mutation that activates

degradation resulted in the interaction of the protein with the ER, perhaps to be worked on by chaperones, before turnover by the proteasome (Table 1).

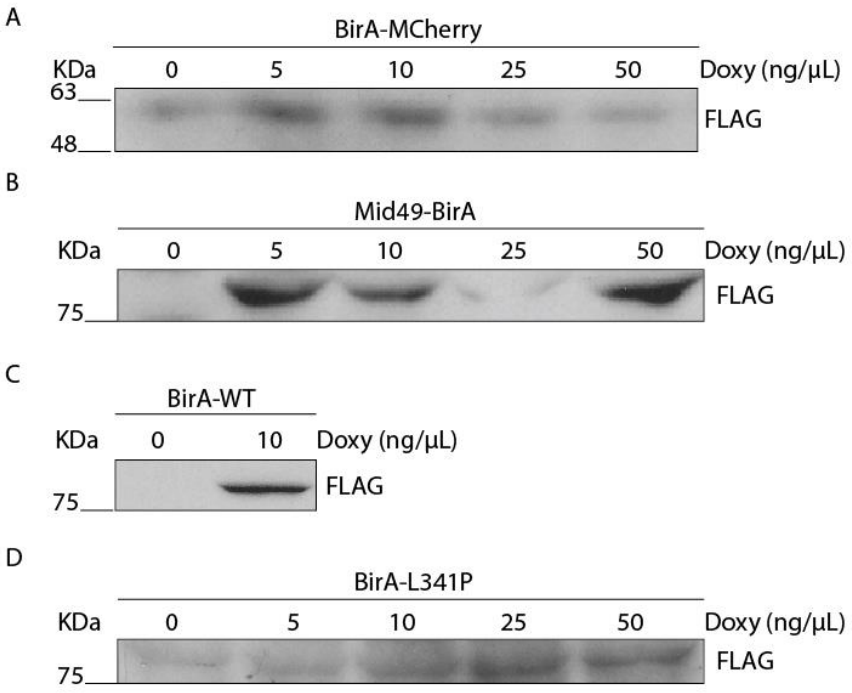


**Figure 1: Induction of BirA recombinant Cell Lines**

HEK 293 cells were grown in DMEM, induced for 24 hours, harvested, and run on 10% SDS-PAGE for analysis. A-D) Doxycycline titration between 0-50 ng/µL of cell line indicated above. Upon even a low concentration of doxycycline, all cell lines showed an increase in protein concentration. Through these analyses, it was decided to induce regularly at 10 ng/µL.

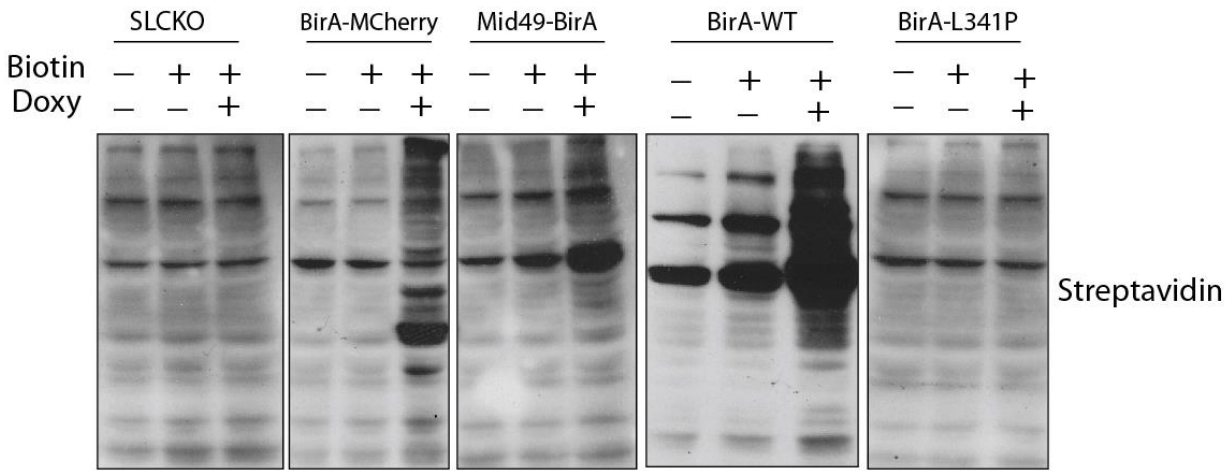


**Figure 2: Biotinylation Tests of BirA Recombinant Cell Lines**

HEK 293 cells were seeded into three different treatments per cell line, treated, harvested, and run on 10% SDS-PAGE for analysis by streptavidin blotting. Here is shown that when induced in the presence of biotin, only the BirA cell lines show an increase in biotinylation. It is postulated that the reason that the BirA-L341P cell line does not show appreciable biotinylation is that the western blot is not sensitive enough to pick up the small amount of biotinylation occurring before the protein is quickly degraded.

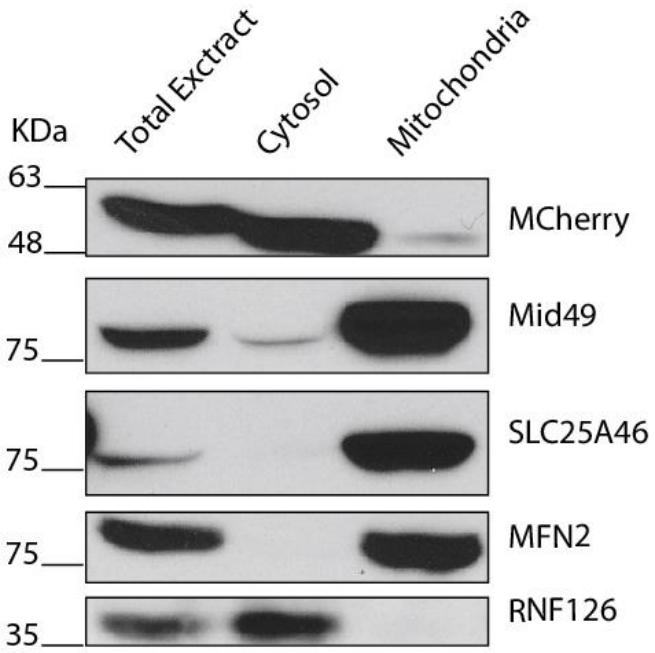


**Figure 3: Subcellular localization of BirA Recombinant Cell Lines**

HEK 293 cells were seeded at high confluence, induced with 10 ng/µL doxycycline for 24 hours, harvested, and separated by total extract, cytosol, and mitochondria. These fractions were run on a 10% SDS-PAGE and blotted for induced protein. All BirA recombinant proteins (excluding the mutant) were found in their appropriate fractions, as compared to the subcellular location controls, MFN2 (mitochondria) and RNF126 (cytosol). Even at high exposure on multiple repeats, the BirA-L341P could not be seen. This could be repeated blotting failure, or a symptom of the high turnover rate of the mutant protein *in vivo*.

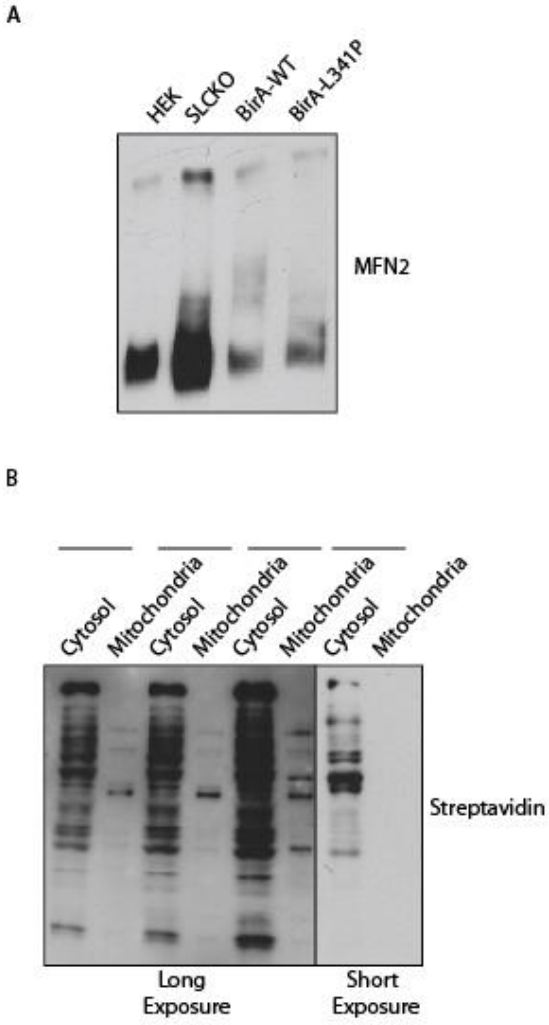


**Figure 4: Functional Assays of BirA Recombinant Cell Lines**

A) Blue native PAGE showing the relative amounts of endogenous MFN2 complexes in different cell lines. It is already established (Steffen et al., 2017) that SLC25A46 loss of function leads to an increase of MFN2 complexes. Here it is shown that BirA-WT rescues native levels of MFN2 upon transfection. B) Streptavidin blot on 10% SDS-PAGE of cells induced in the presence of biotin. Distinct bands can be seen in mitochondrial fraction of BirA-WT cell line, while new high molecular weight bands can be seen in cytosolic fraction of BirA-L341P cell line.

| Description | SLC25A46-WT-A NSAFe5 | SLC25A46-WT-B NSAFe5 | SLC25A46-L341P-A NSAFe5 | SLC25A46-L341P-B NSAFe5 | MID49-A NSAFe5 | MID49-B NSAFe5 | mCherry-A NSAFe5 | mCherry-B NSAFe5 |
|---|---|---|---|---|---|---|---|---|
| Protein disulfide-isomerase | 52.193 | 45.565 | 266.479 | 198.968 | 15.922 | 16.181 | 11.461 | 11.841 |
| 78 kDa glucose-regulated protein | 60.453 | 50.262 | 217.199 | 235.578 | 55.327 | 43.732 | 23.6 | 15.239 |
| Endoplasmin | 69.75 | 53.217 | 204.828 | 150.155 | 40.054 | 25.441 | 7.208 | 7.447 |
| Hypoxia up-regulated protein 1 | 9.894 | 0 | 112.255 | 113.99 | 8.049 | 0 | 0 | 0 |
| Peptidyl-prolyl cis-trans isomerase | 45.759 | 60.873 | 276.897 | 248.096 | 37.226 | 0 | 26.796 | 18.457 |
| 26S protease regulatory subunit | 37.525 | 29.951 | 119.211 | 91.553 | 18.316 | 0 | 30.763 | 36.325 |
| 26S proteasome non-ATPase domain | 104.87 | 78.473 | 277.631 | 195.45 | 63.985 | 54.189 | 56.292 | 42.298 |
| Thioredoxin-like protein 1 | 490.209 | 602.836 | 1189.985 | 1437.069 | 0 | 0 | 0 | 0 |
| Solute carrier family 25 A46 | 1111.358 | 1038.052 | 286.171 | 272.431 | 0 | 0 | 0 | 0 |

**Table 1: Sample of Mass Spectrometry Hits Specific to SLC25A46-L341P**

Here is shown a small sample of the mass spectrometry data from the first biological replicate of the cell line BioID, confirmed by the second biological replicate. The NSAFe5 values is a normalized reading of spectral count that takes into account both protein length and its contribution to the whole list of proteins identified. The proteins highlighted in red are members of the BiP chaperone complex, a well-known ER luminal complex, indicating a presence of the mutant preferentially in the ER. The proteasome subunits demonstrate that the general experimental setup was successful. For the full list of mass spectrometry data, along with initial lists of potentially significant hits, see the Supplementary Materials.

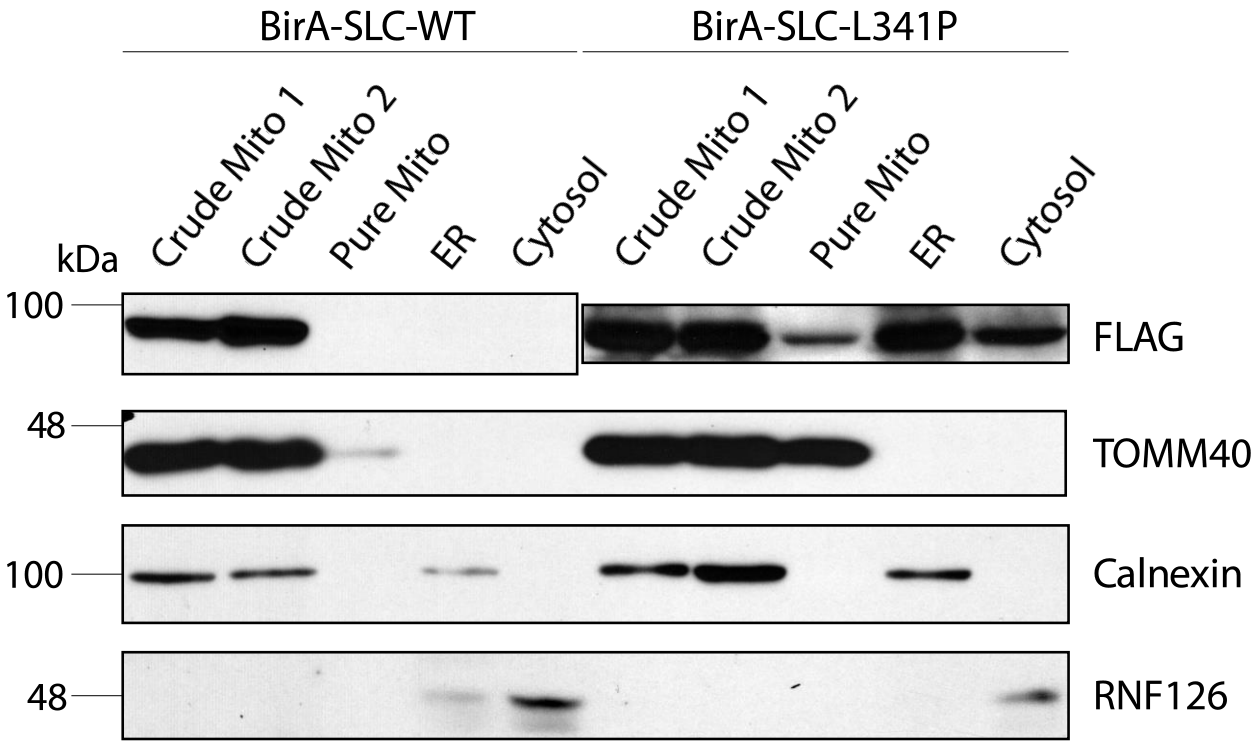


**Figure 5: SLC25A46-L341P is localized to Pure ER**

HEK 293 cells were seeded at high confluence, induced with 10 ng/µL doxycycline for 48 hours, harvested, and separated by cytosol, ER, crude mitochondria, and pure mitochondria. These fractions were run on a 10% SDS-PAGE and blotted for induced protein. These blots demonstrate the presence of SLC25A46-L341P in the ER, preferentially over the mitochondria or cytosol. The ER fraction is pure, demonstrated by the absence of TOMM40 in the fraction. Repeat experiments will be performed to better isolate pure mitochondria. RNF126 – cytosol marker, Calnexin – ER marker, TOMM40 – mitochondrial marker, FLAG – BirA recombinant protein.

## Discussion

Despite its importance in regulating the mitochondria and, by extension, metabolism in the cell, the OMMAD pathway is still not well understood. To date, the only known components of OMMAD are the ubiquitin ligases Parkin, MARCH5, and MULAN, the AAA ATPase p97, and the proteasome and its subunits (Karbowski and Youle, 2011). This reveals the wide variety of components yet to be found, such as the Lys-48-Ub chain recognition machinery, the recruiter of p97, and the chaperones for proteasome delivery. Because of the lack of information of the components, the mechanism of this pathway is still unclear.

The creation and optimization of BioID cell lines of a protein known to be degraded by this mechanism has the potential to identify many of these missing pieces. We have demonstrated that we have created such cell lines. By biotinylating all proximal proteins, the BirA recombinant proteins allowed convenient pull down of all transiently interacting proteins through streptavidin affinity purification. These cell lines are doxycycline inducible at low concentrations, capable of biotinylation, and has correctly localized recombinant proteins (Fig. 1-3). Following successive BioID activations and subsequent affinity purification, a comprehensive mass spectrometry list has been obtained that was analyzed for information regarding the OMMAD pathway (Table 1).

The mass spectrometry analysis revealed a pattern of biotinylation in the ER that was specific to mutant SLC25A46 (Table 1). The BiP chaperone complex seemed to be preferentially associated with the mutant, indicating a possible attempt by the complex to refold the protein before it eventually is destroyed by ERAD, or the complex may simply be functioning as the recognition machinery. Given that SLC25A46 is degraded by an ubiquitin-dependent mechanism, it is reasonable to suggest that since it is found in the ER that it will be degraded by

ERAD, the ubiquitin-dependent degradation system of the ER (Steffen et al., 2017; Ruggiano et al., 2014). The presence of the mutant in the ER preferentially has been confirmed by Percoll gradient centrifugation followed by western blotting (Fig. 5).

The relationship between SLC25A46 and its degradation in the ER indicates close proximity and perhaps even a functional interaction, suggesting the inclusion of SLC25A46 into the mitochondria-associated membrane (MAM) complex. This is supported by recent proteomic analysis of the MAM that found SLC25A46 in both the mitochondrial and ER fractions, indicating it as a potential interactor (Ma et al., 2017). In general, this makes sense of some of the divergent explanations of SLC25A46's function. It has been confirmed to be involved in mitochondrial dynamics, and implicated to be important for lipid transfer (Steffen et al., 2017; Janer et al., 2016). These are functions well-known to be associated with the MAM, where mitochondrial fission is initiated and where newly synthesized lipids from the ER are transported to the mitochondrial membrane (Phillips et al., 2016; Wirtz et al., 1968). While not necessarily directly involved in these processes, SLC25A46 may be functioning as a structural protein, recruiting the canonical members of this complex, and in its absence, hindering lipid exchange and mitochondrial dynamics.

It is important to recognize the limitations of the method we have used to assay the turnover mechanism of SLC25A46. Despite the undisputed significance of some of the hits found in the BiP chaperone complex and of ERAD, initial attempts at quantification have revealed that many of the supposed hits may be statistically insignificant. This could be explained by the presence of a basal level of wildtype SLC25A46 found in the ER which is amplified in the SLC25A46-L341P fraction in the absence of it stably labeling in the mitochondria. To better characterize the data collected, more confirmation experiments should

be performed. Among them, another Percoll gradient centrifugation experiment should be performed comparing normal cell conditions to those with a P97 inhibitor (an inhibitor of the UPS), which would reveal the subcellular compartment of the mutated protein aggregates. If the protein accumulates in the ER, it would confirm the conclusions of this paper. In addition, immunoprecipitations should be performed on wild type and mutant SLC25A46 to determine if these ER contacts are in fact robust, or merely transitory associations of proximity.

Considering the importance of the mitochondria to the functioning of every cell, and by extension every human, the elucidation of its processes is of immediate importance. This is especially true for the OMMAD pathway, because it controls the proteomic makeup of the OM and the health of the organelle. By understanding SLC25A46 degradation, we have a larger picture of the mechanism of this pathway, and of the function of mitochondria.

## References


Abrams, A.J., Hufnagel, R.B., Rebelo, A., Zanna, C., Patel, N., Gonzalez, M.A., Campeanu, I.J., Griffin, L.B., Groenewald, S., Strickland, A.V., et al. (2015) Mutations in SLC25A46, encoding a UGO1-like protein, cause an optic atrophy spectrum disorder. *Nature Genetics* 47, 926-932.

Adusumilli R, Mallick P. (2017) Data Conversion with ProteoWizard msConvert. *Methods Mol Biol*. 1550, 339-68.

Burr, M.L., van den Boomen, D.J., Bye, H., Antrobus, R., Wiertz, E.J., and Lehner, P.J. (2013) MHC class I molecules are preferentially ubiquitinated on endoplasmic reticulum luminal residues during HRD1 ubiquitin E3 ligase mediated dislocation. *Proc. Natl. Acad. Sci. USA* 110, 14290–14295

Chen, H., Detmer, S.A., Ewald, A.J., Griffin, E.E., Fraser, S.E, and Chan, D.C. (2003) Mitofusins Mfn1 and Mfn2 coordinately regulate mitochondrial fusion and are essential for embryonic development. *Journal of Cell Biology* 160, 189-200.

Choi M, Chang CY, Clough T, Broudy D, Killeen T, MacLean B, Vitek O. (2014) MSstats: an R package for statistical analysis of quantitative mass spectrometry-based proteomic experiments. *Bioinformatics*. 30, 2524-6.

Dudek, J., Rehling, P., and van der Laan, M. (2013) Mitochondrial protein import: Common principles and physiological networks. *Biochimica et Biophysica Acta* 1833, 274-285.

Janer A, Prudent J, Paupe V, Fahiminiya S, Majewski J, Sgarioto N, Des Rosiers C, Forest A, Lin ZY, Gingras AC, et al. (2016) SLC25A46 is required for mitochondrial lipid homeostasis and cristae maintenance and is responsible for Leigh syndrome. *EMBO Mol Med. 8*, 685-829.

Kall L, Canterbury JD, Weston J, Noble WS, MacCoss MJ. (2007) Semi-supervised learning for peptide identification from shotgun proteomics datasets. *Nat Methods*. 4, 923-5.

Kalousek F., Isaya G., Rosenberg L. E. (1992) Rat liver mitochondrial intermediate peptidase (MIP): purification and initial characterization. *EMBO J* 11, 2803–2809

Karbowski, M. and Youle, R.J. (2011) Regulating mitochondrial outer membrane proteins by ubiquitination and proteasomal degradation. *Curr. Opin. Cell Biol*. 23, 476-482.

Kim S, Pevzner PA. (2014) MS-GF+ makes progress towards a universal database search tool for proteomics. *Nat Commun*. 5, 5277.

Kleizen, B., and Braakman, I. (2004) Protein folding and quality control in the endoplasmic reticulum. *Current Opinion in Cell Biology* 16, 343-49.

Koppen, M., & Langer, T. (2007) Protein Degradation within Mitochondria: Versatile Activities of AAA Proteases and Other Peptidases. *Critical Reviews in Biochemistry and Molecular Biology* 42, 221-42.

Lenaz, G. (1998). Role of mitochondria in oxidative stress and ageing. *Biochim. Biophys.Acta* 1366, 53-67.

Liesa, M., and Shirihai, O.S. (2013) Mitochondrial Dynamics in the Regulation of Nutrient Utilization and Energy Expenditure. *Cell Metabolism* 17, 491-506.

Ma, J. H., Shen, S., Wang, J. J., He, Z., Poon, A., Li, J., Qu, J., and Zhang, S. X. (2017). Comparative Proteomic Analysis of the Mitochondria-associated ER Membrane (MAM) in a Long-term Type 2 Diabetic Rodent Model. Scientific Reports, 7, 2062.

Neutzner, A., Youle R.J., and Karbowski, M. (2007) Outer mitochondrial membrane protein degradation by the proteasome. *Novartis Found Symp* 287, 4-14.

Ou W. J., Okazaki H., Omura T. (1989) Purification and characterization of a processing protease from rat liver mitochondria. *EMBO J* 8, 2605–2612

Palmieri, F. (2014) Mitochondrial transporters of the SLC25 family and associated diseases: a review. *J Inherit Metab Dis. 37*, 565-575.

Phillips, M.J., and Voeltz, G.K. (2016) Structure and function of ER membrane contact sites with other organelles. *Nature Reviews Molecular Cell Biology* 17, 69–82.

Pusnik, M., Charriere, F., Maser, P., Waller, R.F., Dagley, M.J., Lithgow, T., and Schneider, A. (2009) The Single Mitochondrial Porin of Trypanosoma brucei is the Main Metabolite Transporter in the Outer Mitochondrial Membrane. *Mol. Biol. Evol.* 26, 671–680.

Reiter L, Rinner O, Picotti P, Huttenhain R, Beck M, Brusniak MY, Hengartner MO, Aebersold R. (2011) mProphet: automated data processing and statistical validation for large-scale SRM experiments. *Nat Methods*. 8, 430-5.

Ruggiano, A., Foresti, O., and Carvalho, P. (2014) ER-associated degradation: Protein quality control and beyond. *J Cell Biol* 204, 869-879.

Schilling B, Rardin MJ, MacLean BX, Zawadzka AM, Frewen BE, Cusack MP, Sorensen DJ, Bereman MS, Jing E, Wu CC, Verdin E, Kahn CR, Maccoss MJ, Gibson BW. (2012) Platform-independent and label-free quantitation of proteomic data using MS1 extracted ion chromatograms in skyline: application to protein acetylation and phosphorylation. *Mol Cell Proteomics*. 11, 202-14.

Senko MW, Remes PM, Canterbury JD, Mathur R, Song Q, Eliuk SM, Mullen C, Earley L, Hardman M, Blethrow JD, Bui H, Specht A, Lange O, Denisov E, Makarov A, Horning S, Zabrouskov V. (2013) Novel parallelized quadrupole/linear ion trap/Orbitrap tribrid mass

spectrometer improving proteome coverage and peptide identification rates. *Anal. Chem*. 85, 11710-4.

Serang O, MacCoss MJ, Noble WS. (2010) Efficient marginalization to compute protein posterior probabilities from shotgun mass spectrometry data. *J Proteome Res*. 9, 5346-57.

Steffen, J., Vashisht, AA, Wan, J., Jen, JC, Claypool, SM, Wohlschlegel, JA, and Koehler, CM. (2017) Rapid degradation of mutant SLC25A46 by the ubiquitin-proteasome system results in MFN1/2 mediated hyperfusion of mitochondria. *Mol. Biol. Cell* 28, 600-12.

Van Dyck L, Langer T. (1999) ATP-dependent proteases controlling mitochondrial function in the yeast Saccharomyces cerevisiae. *Cell Mol Life Sci* 55, 825–842.

Wai, T. and Langer, T. (2016) Mitochondrial Dynamics and Metabolic Regulation. *Trends in Endocrinology & Metabolism* 27, 105-117.

Wan, J, Steffen, J, Yourshaw, M, Mamsa, H, Andersen, E, Rudnik-Schöneborn, S, Pope, K, Howell, KB, McLean, CA, Kornberg, AJ, Joseph, J, Lockhart, PJ, Zerres, K, Ryan, MM, Nelson, SF, Koehler, CM, and Jen, JC (2016) Loss of function of SLC25A46 causes lethal congenital pontocerebellar hypoplasia. *Brain* 139, 2877-2890.

Wirtz, K. W. and Zilversmit, D. B. (1968) Exchange of phospholipids between liver mitochondria and microsomes in vitro. *J. Biol. Chem*. 243, 3596–3602.

Wohlschlegel JA (2009) Identification of SUMO-conjugated proteins and their SUMO attachment sites using proteomic mass spectrometry. *Methods Mol Biol*. 497, 33-49.

Young L., Leonhard K., Tatsuta T., Trowsdale J., Langer T. (2001) Role of the ABC transporter Mdl1 in peptide export from mitochondria. *Science* 291, 2135–2138.